Journal of Zhejiang University-SCIENCE C (Computers & Electronics)
ISSN 1869-1951 (Print); ISSN 1869-196X (Online)
www.zju.edu.cn/jzus; www.springerlink.com
E-mail: jzus@zju.edu.cn

Centroid-based sifting for empirical mode decomposition*

Hong HONG†1, Xin-long WANG[1], Zhi-yong TAO[1], Shuan-ping DU[2]

([1]*Key Laboratory of Modern Acoustics and Institute of Acoustics, Nanjing University, Nanjing 210093, China*)

([2]*State Key Laboratory of Ocean Acoustics, Hangzhou Applied Acoustics Research Institute, Hangzhou 310012, China*)

†E-mail: hongnju@gmail.com

Received Feb. 25, 2010; Revision accepted May 20, 2010; Crosschecked Dec. 30, 2010

Abstract: A novel sifting method based on the concept of the 'local centroids' of a signal is developed for empirical mode decomposition (EMD), with the aim of reducing the mode-mixing effect and decomposing those modes whose frequencies are within an octave. Instead of directly averaging the upper and lower envelopes, as suggested by the original EMD method, the proposed technique computes the local mean curve of a signal by interpolating a set of 'local centroids', which are integral averages over local segments between successive extrema of the signal. With the 'centroid'-based sifting, EMD is capable of separating intrinsic modes of oscillatory components with their frequency ratio ν even up to 0.8, thus greatly mitigating the effect of mode mixing and enhancing the frequency resolving power. Inspection is also made to show that the integral property of the 'centroid'-based sifting can make the decomposition more stable against noise interference.

Key words: Sifting, Empirical mode decomposition (EMD), Mode mixing effect, Frequency resolution, Local centroids, Noise resistance

doi:10.1631/jzus.C1000037 **Document code:** A **CLC number:** TP391.4

1 Introduction

Time frequency analysis has been one of the major topics in modern signal processing, and has become an indispensable tool. Among the various techniques for time-frequency analysis are the spectrogram and the Wigner distribution (Cohen, 1989; Hlawatsch and Boudreaux-Bartels, 1992), both of which have been intensively studied and most widely applied in diverse areas of engineering science in recent decades. The prerequisites for applications of these techniques are the linearity and, at least short time, stationarity for signals to be analyzed, which confines the applicability in many real situations. In fact, a vast number of deterministic systems and associated signals are intrinsically nonlinear or even exhibit chaoticity, implying the impertinence of the mathematical view of expanding them as the linear superposition of a series of a priori orthogonal base functions. On the other side, the complexity of real systems and the unpredictability of external disturbances and fluctuations usually render the generated signals highly nonstationary, at least on some long time scales. A typical example is the human voicing system and the produced speech, which manifests high stochasticity, e.g., between transitions of successive syllables. All these necessitate some conceptually new time-frequency techniques devised specifically for processing signals that are both nonlinear and nonstationary. The recently developed Hilbert-Huang transform (HHT) (Huang *et al.*, 1998) seems sufficient for the purpose.

The essence of HHT is the empirical mode decomposition (EMD) by means of a process called sifting. With EMD, any signal, whether linear or nonlinear, is disintegrated into a sequence of the so-called intrinsic mode functions (IMF) that characterize the underlying dynamics and evolution of the system generating the signal. Acting as base

* Project supported by the National Natural Science Foundation of China (No. 10574070) and the State Key Laboratory Foundation of China (No. 9140C240207060C24)

functions in decomposition, IMFs seem to be the counterpart of a predefined set of orthogonal functions like those used in Fourier analysis, but it can well reflect local temporal variations, and are fully data or signal specific. These features further make HHT not only capable of coping with nonstationary signals, but also highly adaptive in general signal processing (Huang and Wu, 2007). Although still in its developing state, HHT has already demonstrated its remarkable power in a number of applications (Huang *et al.*, 2001; Liang *et al.*, 2000; Schlurmann *et al.*, 2001; Messina, 2009).

However, aside from the lack of a perfect mathematical foundation, the HHT methodology also faces a number of problems to be resolved in algorithm implementation and application.

One of the major problems is mode mixing or scale mixing, by which a decomposed IMF may contain more than one intrinsically different oscillation of distinct time scales, directly violating the belief that an IMF characterizes the unique dynamic behaviors on a particular time scale. The mode mixing due to intermittent interference of considerably high frequency can easily be handled, say, by introducing an additional criterion in sifting, as was discussed by Huang *et al.* (1999). The more difficult to handle is the mixing between oscillatory modes, with their frequency ratios ν greater than 0.6 and less than $1/0.6$ (Datig and Schlurmann, 2004; Rilling and Flandrin, 2008). To break through this limitation, a number of approaches have been undertaken, for example, the use of the alternate extrema for the envelopes (Huang *et al.*, 1999), the bandwidth criterion for IMF (Xuan *et al.*, 2007), the masking signal (Deering and Kaiser, 2005; Deering, 2006; Senroy *et al.*, 2007; Laila *et al.*, 2009; Messina, 2009), the heuristic search optimization approach (Kopsinis and McLaughlin, 2008a), and doubly-iterative sifting (Kopsinis and McLaughlin, 2008b), all showing their advantages in alleviating the effect. However, some of these approaches need to assume a set of a priori operations before decomposition, which would spoil the adaptivity that the original EMD method features. Also, the limited improvement of these approaches sometimes does not satisfy practical applications.

Another non-trivial problem is relevant to the robustness of the EMD algorithm against noise disturbance, originated from either computation or some external sources. The currently available sifting methods depend highly on the detection of characteristic points of a signal in order to estimate the local mean curve, which is actually the signal constituents that vary on some longer time scales. This might cause serious problems like susceptivity to the error of detection, the low ability of noise resistance, etc., leading to instability of sifting iterations, and thus, resulting in incorrect decomposition or even creating spurious IMFs or totally meaningless IMFs.

In an attempt to reduce the mode-mixing effect and construct a stable decomposition, here we propose an alternative sifting method for EMD by introducing the concept of 'local centroids' of a signal and employing the 'local centroids' for estimating the local mean curve.

2 Problem

EMD is based on the reconstruction of the local mean $\bar{x}(t)$ of a signal $x(t)$, a concept that is highly relevant to characteristic time scales implicated in the signal. A truly local mean $\bar{x}(t)$ should contain only those components of $x(t)$ that vary on longer time scales than the IMF just being extracted. Then there raises a critical issue: how to obtain an adequate $\bar{x}(t)$ in practice?

In the original EMD (Huang *et al.*, 1998), the sifting retains the component of $x(t)$ with time scale of the order of time lapses between successive extrema of $x(t)$, while the curve of $\bar{x}(t)$ was assumed to be the arithmetic average of the lower and upper envelopes which are computed by interpolating minima and maxima of $x(t)$, respectively. Estimating $\bar{x}(t)$ in this way may cause problems like undershoot, overshoot, instabilities to noise, and error of detection of extrema. In particular, the sifting would render it impossible to decompose intrinsically different modes whose frequencies fall in an octave.

To illustrate this, we take a classic nonlinear model, the Duffing equation, as an example:

$$\frac{\mathrm{d}^2x}{\mathrm{d}t^2}+x+\epsilon x^3=\gamma\cos(\omega_f t), \tag{1}$$

where ϵ is a nonlinear parameter, and γ and ω_f are the driving amplitude and angular frequency, respectively. By integrating Eq. (1) with the standard Runge-Kutta algorithm, the numeric solution can be easily obtained. Here we set $\epsilon=-1.1$, $\gamma=0.02$, and $\omega_f=0.45$, so that the oscillator that is subject to a

nonlinear restoration by a soft spring not only is of high nonlinearity, but also is strongly forced. Fig. 1 shows the time waveform evolving from $x(0) = 0.9$ and $x'(0) = 0$, and its FFT spectrum $X(\omega)$. From the spectrum one can read that the nonlinear eigenfrequency $\omega_0 \approx 0.64$, considerably smaller than the linear one at $\omega = 1$, indicating that the forced motion of the oscillator is highly nonlinear.

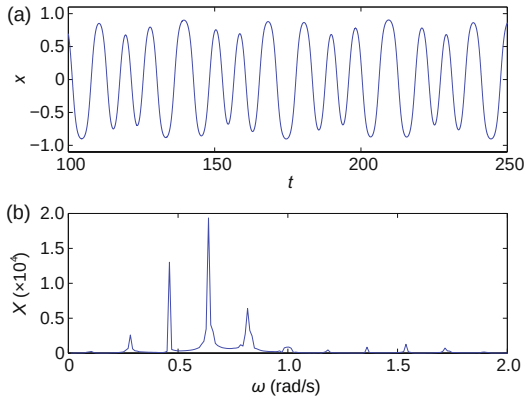

Fig. 1 Response of the Duffing oscillator (a) and its fast Fourier tranform (FFT) spectrum (b)

Undoubtedly, the two dominant spectral peaks of comparable strengths are distinct oscillatory modes, one being the eigenmode of the nonlinear oscillator of frequency $\omega = \omega_0$, and the other the forced oscillation of frequency $\omega = \omega_f$. One perhaps needs to separate them from each other for further analysis. Nevertheless, as shown in Fig. 2, EMD fails to do so. The first decomposed, IMF_1, is almost identical to the original $x(t)$, both in waveform and spectrum (omitted here). The second, IMF_2, much smaller in amplitude, has the spectrum dominated neither by the ω_0 nor by the ω_f mode. An FFT analysis turns out that the dominant spectral peak of IMF_2 is located at $\omega = 2\omega_f - \omega_0 = 0.26$, a subharmonic induced by nonlinear coupling between the $2\omega_f$ superharmonic and the ω_0 eigenmode. The third, IMF_3, with even lower frequency, is actually negligible.

For this example, the frequency ratio of the two dominant components $\nu = \omega_f/\omega_0 \approx 0.7031$, which is within an octave. In fact, in EMD $x(t)$ is regarded as a single IMF which is almost indecomposable. This not only limits the frequency resolving power of the decomposition, but also induces ambiguity in uncovering the associated physics. It shows the necessity

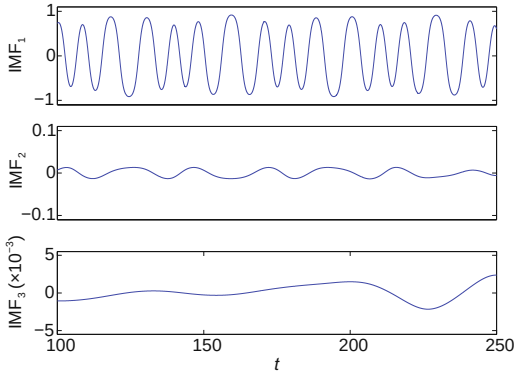

Fig. 2 Decomposition of the Duffing signal by the original empirical mode decomposition (EMD)

of an improved or alternative EMD method to reduce the mode-mixing effect.

3 Local centroids and sifting

The key step for the IMF decomposition is the estimation of the local mean curve $\bar{x}(t)$ of a signal $x(t)$. The concept of 'local mean' is somewhat bewildering. Mathematically it should exist at any time t, reflecting the temporal fluctuation of the varying background on which the fast oscillation rides. On the other hand, it is relevant to a time scale τ that is being considered and analyzed; that is, it should vary much more slowly such that it nearly keeps constant on the time scale τ on the order of the period of fast oscillation. Bearing in mind this subtlety, we realize that $\bar{x}(t)$ could be formulated in such a way as to assume a kind of average over the time scale τ. Then it is quite natural and seems more reasonable for $\bar{x}(t)$ to be estimated by the local 'centroid' of the curve of $x(t)$ within the time scale τ.

Let $(t_k,\ x_k)$ denote the kth local extremum of $x(t)$, with $\cdots < t_{k-1} < t_k < t_{k+1} < \cdots$ $(k = 0, 1, 2, \cdots)$. The sequence, $(t_k,\ x_k)$, consists of interlaced minima and maxima, for instance, the minima with odd k and the maxima with even k. Accordingly, $x(t)$ is divided into a sequence of signal segments C_k, $t \in (t_k, t_{k+1})$, for $k = 0, 1, 2, \cdots$, each being monotonically increasing or decreasing in time. Then, for each C_k, we can define its 'mass center' or 'centroid', $(\bar{t}_k, \bar{x}_k)$, a concept directly borrowed from classic mechanics:

$$(\bar{t}_k, \bar{x}_k) = \frac{1}{l_k}\int_{C_k}(t, x)\mathrm{d}s, \quad l_k = \int_{C_k}\mathrm{d}s, \qquad (2)$$

as if the segment C_k of length l_k, from a minimum (maximum) (t_k, x_k) to the nearest neighboring maximum (minimum) (t_{k+1}, x_{k+1}) on the (t, x) plane, were mass-bearing, with uniform mass density in the 2D space. Explicitly, Eq. (2) can be expressed as

$$\begin{cases} \bar{x}_k = \dfrac{1}{l_k}\displaystyle\int_{t_k}^{t_{k+1}} x(t)\sqrt{1+x'(t)^2}\mathrm{d}t, \\ \bar{t}_k = \dfrac{1}{l_k}\displaystyle\int_{t_k}^{t_{k+1}} t\sqrt{1+x'(t)^2}\mathrm{d}t, \end{cases} \tag{3}$$

with

$$l_k = \int_{t_k}^{t_{k+1}} \sqrt{1+x'(t)^2}\mathrm{d}t.$$

We thus obtain a sequence of local 'centroids', $(\bar{t}_k, \bar{x}_k)$, $k = 0, 1, 2, \cdots$, for $x(t)$. Obviously the 'centroids' $(\bar{t}_k, \bar{x}_k)$ thus defined should locally reflect the mean values of monotonically changing segments C_k of $x(t)$. By interpolating the discrete set of data, e.g., by the cubic spline, we obtain a well-behaved smooth curve which is taken as the local mean curve $\bar{x}(t)$. The remaining work for sifting is exactly the same as originally developed by Huang. We thus refer readers to Huang *et al.* (1998) for details.

Note that, for a discrete signal, after a search for extrema (minima and maxima), we can use the numerical methods such as the trapezoid rule to calculate Eq. (3) easily, with the involved derivative $x'(t)$ being numerically evaluated simply by, say, the mid-point formula.

To illustrate, let us return to the signal $x(t)$ that is produced from the Duffing equation (1), as has just been addressed in the preceding section. The local 'centroids' calculated through Eq. (3) are shown in Fig. 3. Also presented in the figure are the local mean curves obtained by interpolating the 'centroids' and by averaging the lower and upper envelopes of $x(t)$, respectively. The cubic spline is used for all interpolations. With the envelope averaging method, we obtain a local mean curve that almost vanishes in the whole time span, showing the high symmetry of the lower and upper envelopes. With the 'centroid'-based method, however, we obtain a local mean curve $\bar{x}(t)$ that fluctuates at the forcing frequency ω_f. Hence, the local 'centroids' can reflect more subtly the local variation of the highly nonlinear signal. A closer look at the figure shows that centroids may even not lie on, but deviate slightly from, the signal curve, reflecting the barely detectable asymmetry of the Duffing oscillation that is induced by the nonlinear coupling of two distinct oscillatory modes. This fine structure of asymmetry, however, cannot be captured by envelope averaging, since the lower and upper envelopes are almost symmetric with respect to $x = 0$. For signals of higher non-symmetry, centroids may deviate more observably from the signal curve. We therefore anticipate better decomposition with the 'centroid'-based sifting technique.

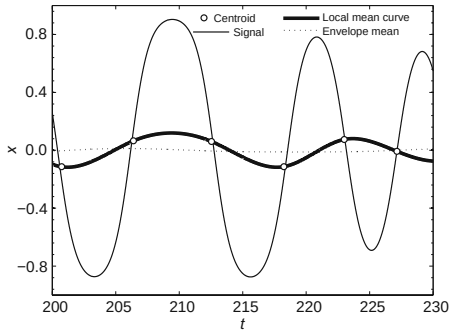

Fig. 3 Local 'centroids' of the Duffing signal $x(t)$ and the interpolated local mean curve. The dotted line is the local mean curve resulting from averaging the upper and lower envelopes of the signal

In contrast to the results shown in Fig. 2, we present in Fig. 4 the decomposition via 'centroid'-based sifting. We now see that IMF_1 is almost the intrinsic mode of the Duffing oscillator, albeit it contains minor components of higher frequencies resulting from nonlinear coupling. IMF_2 now turns out the pure forced oscillation of frequency $\omega = \omega_f = 0.45$, with an amplitude comparable to that of IMF_1, much consistent with the spectrum as displayed in Fig. 1. As to IMF_3, we find it to be the subharmonic of frequency $2\omega_f - \omega_0$, which is induced by the nonlinear interaction between the superharmonics of frequency $2\omega_f$ and the eigenmode of frequency ω_0. The primary success in decomposing the nonlinear signal is just a first indication of the superiority of 'centroid'-based sifting over that based on the average of the lower and upper envelopes.

4 Performance verification and comparison

To see how the centroid-based sifting method reduces the mode-mixing effect and improves the frequency resolution, let us investigate the decomposition of the simplest model consisting of a two-tone

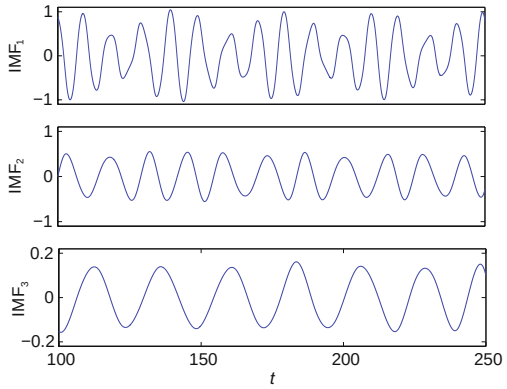

Fig. 4 Decomposition of the Duffing signal using the centroid-based method

harmonic given by

$$x(t) = x_1(t)+x_2(t) = \sin(2\pi t)+a\sin(2\pi\nu t+\psi). \quad (4)$$

When $\nu \in [0,1]$ and $a \in [0.1,100]$, the term $\sin(2\pi t)$ is the higher frequency component and $a\sin(2\pi\nu t+\psi)$ is the lower frequency one. To measure the quality of decomposition, we use the cross-correlation coefficients as defined by

$$r_i = \frac{C(x_i, \mathrm{IMF}_i)}{\sqrt{\sigma(x_i)\sigma(\mathrm{IMF}_i)}}, \quad i = 1,2, \qquad (5)$$

where $C(X,Y)$ is the covariance between X and Y, and $\sigma(X)$ is the variance of X. Only if both $r_1 > 0.95$ and $r_2 > 0.95$ do we regard the decomposition as being successful. By varying $\nu \in [0,1]$ and $a \in [0.1,100]$, with a ferret-like survey, we finally obtain in the (a,ν)-plane a diagram as shown in Fig. 5, which gives the (a,ν)-region (the white area) within which the decomposition is successful. Also indicated in the diagram is the critical cutoff frequency ratio, $\nu \approx 0.6$ (for $a \approx 1$), above which the original EMD fails to separate two harmonics. As can be seen, the centroid-based sifting breaks through the limit and extends the cutoff up to $\nu \approx 0.8$ for $a = O(1)$. Note that in constructing the mean curve $\bar{x}(t)$ here and below, cubic spline is always adopted for interpolating discrete data, not only for our centroid-based method, but also for the original EMD.

Then we consider a slight extension to the above example, the decomposition of a three-tune signal, $x(t) = x_1(t)+x_2(t)+x_3(t)$, with $x_1 = 0.9\sin(0.13t)$, $x_2 = 0.8\sin(0.08t)$, $x_3 = \sin(0.05t)$, $t \in [0,3000]$. To avoid the possible boundary effect, we perform the

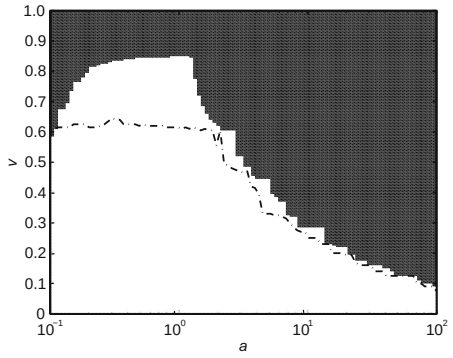

Fig. 5 Performance measure of two-component signal decomposition using the centroid-based method. The white region stands for the well-separated domain. Also depicted is the dashed-dotted line below which the decomposition is successful by the original EMD

decomposition in a longer time span ($t \in [0,3000]$) than displayed in Figs. 6 and 7. In Fig. 6, the results by the original EMD are disappointing. Mode mixing between x_1 and x_2 ($\nu = 0.62$) and between x_2 and x_3 ($\nu = 0.63$) appear so much severe that $\mathrm{IMF}_1 \neq x_1(t)$, $\mathrm{IMF}_2 \neq x_2(t)$, and $\mathrm{IMF}_3 \neq x_3(t)$, and the result is totally unacceptable. Fig. 7 presents the IMFs decomposed by the 'centroid'-based method and by the refined EMD (R-EMD) (Laila *et al.*, 2009). Although the intrinsic frequencies of IMFs by R-EMD were consistent with $x_i(t)$ ($i = 1,2,3$), there exist the amplitude leakage of IMF_1 and IMF_2. By contrast, the results from the 'centroid'-based method in Fig. 7, $\mathrm{IMF}_1 \approx x_1(t)$, $\mathrm{IMF}_2 \approx x_2(t)$, and $\mathrm{IMF}_3 \approx x_3(t)$, show the remarkable success of the centroid-based sifting.

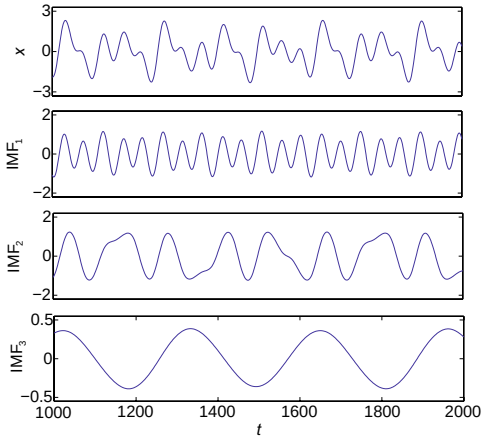

Fig. 6 Decomposition of the three-component signal using the original EMD

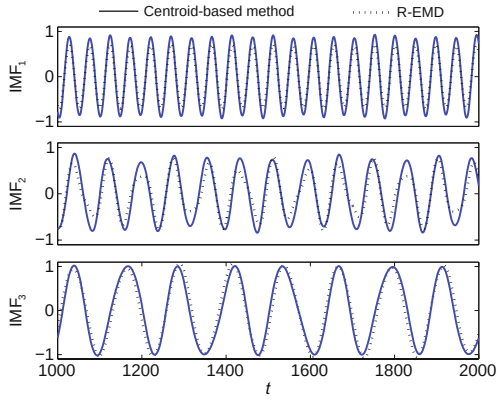

Fig. 7 Decompositions of the three-component signal using the 'centroid'-based method and R-EMD

Lastly, we consider a more complex signal $x(t)$ (Fig. 8a) that consists of a simple harmonic $x_1(t)$ of constant frequency f_1 and amplitude a_1, $x_1(t) = a_1\cos(2\pi f_1 t)$, and a sinusoid $x_2(t)$ of constant frequency $f_2 = 0.5f_1$ but with a linearly increasing amplitude $a_2(t)$, $x_2 = a_2(t)\cos(2\pi f_2 t)$, with $a_1 = 1$, $f_1 = 2f_2 = 1/25$, $a_2(t) = 0.5 + (14.5/30\,000)t$. This example demonstrates the ability of the 'centroid'-based method in extracting the faster oscillatory signal $x_1(t)$ in the presence of a drifting background of lower frequency (Kopsinis and McLaughlin, 2008b). For comparison, we also show the results by the original EMD and R-EMD. The performance can be measured by the maximal amplitude ratio, a_2/a_1, up to which the decomposition fails. The extractions by the three methods are shown in Figs. 8b–8d. We observe that the ratio for the new method is about 5, almost doubling the values of about 3 by the R-EMD and 3.5 by the original EMD.

5 Noise resistance

We expect that the integral property of the 'centroid'-based sifting can better endure noise interference than the original EMD. We demonstrate this also by decomposing a noise-contaminated signal that consists of two simple harmonics plus a Gaussian white noise, i.e.,

$$x(t) = x_1(t) + x_2(t) + \varepsilon(t), \quad t \in [0, 3000], \qquad (6)$$

with

$$x_1(t) = \sin(0.15t), \quad x_2(t) = \sin(0.07t), \qquad (7)$$

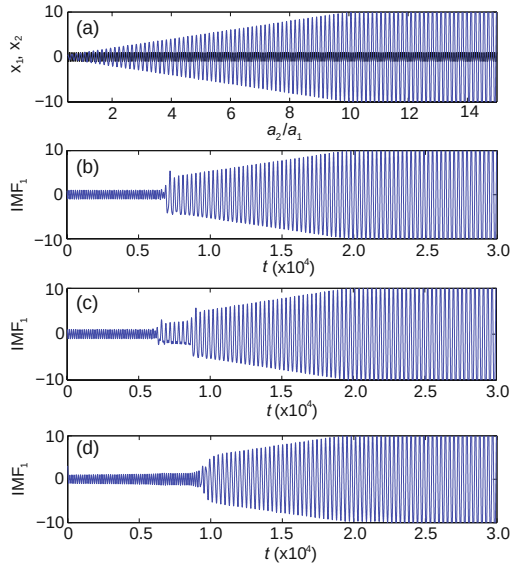

Fig. 8 Extraction of the fast oscillatory component $x_1(t)$ from $x(t)$: (a) Parametric plots of x_1 and x_2 (the linearly growing one); (b) IMF_1 extracted by the original EMD; (c) IMF_1 by the R-EMD; (d) IMF_1 by the 'centroid'-based method

and $\varepsilon(t)$ an additive Gaussian white noise. In the case of $\varepsilon(t) = 0$, since the frequency ratio ν of the two harmonics takes the value of 0.47, both original EMD and 'centroid'-based one can decompose $x(t)$ perfectly into two IMFs, here IMF_1 and IMF_2, which approximate well to $x_1(t)$ and $x_2(t)$, respectively. With the introduction of additive noise, the performances of both methods are quite different. To measure this, we calculate the cross-correlation coefficients r_i, as defined in Eq. (5), between x_i $(i = 1, 2)$ and the corresponding IMF. As the IMFs that approximate x_1 and x_2 are no longer IMF_1 and IMF_2 for the noisy signal, but shift to the higher order IMFs, IMF_j with indices $j > 2$, we must first pick up those that best approximate x_1 and x_2 before calculating r_i. Fig. 9 shows how r_1 (Fig. 9a) and r_2 (Fig. 9b) vary as the signal-to-noise ratio (SNR) decreases from 20 dB (low noise level) to 0 dB (high noise level). We find that, for high SNR, say, SNR>10 dB, both methods can achieve essentially the same results. Nevertheless, for SNR<10 dB, the performance of the original EMD degrades drastically, while the 'centroid'-based method can achieve acceptable decomposition, even for SNR as low as 5 dB, considerably enhancing the ability of resisting against noise interference. Note that here and afterwards, since the R-EMD is sensitive to noise disturbance, the performance of this method is excluded in this section.

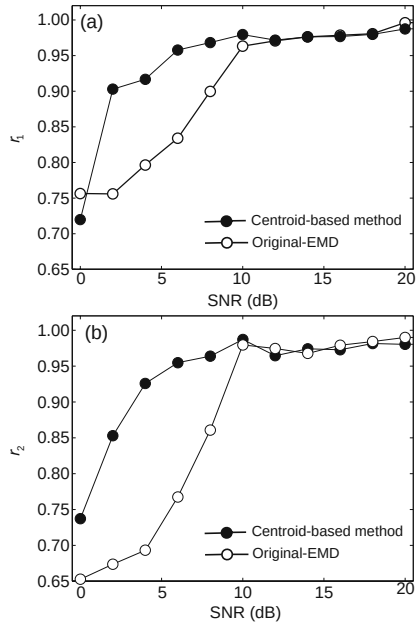

Fig. 9 Performance comparison of noise resistance. (a) The cross-correlation coefficients r_1 between $x_1(t)$ and the corresponding IMF; (b) r_2 between $x_2(t)$ and the corresponding one

For the similar signal $x(t)$ as given in Eq. (6) but with

$$x_1(t)=\sin(0.1t),\quad x_2(t)=\sin(0.07t), \tag{8}$$

since $\nu=0.7$, the original EMD cannot decompose x_1 or x_2 out of the composite x, even if $\varepsilon=0$. However, the 'centroid'-based method is still able to accomplish this. We have also calculated the cross-correlation coefficients r_i versus SNR (Fig. 10). The results show that the decomposition is acceptable ($r_i\approx 0.95$), even if SNR is as low as 5 dB or so.

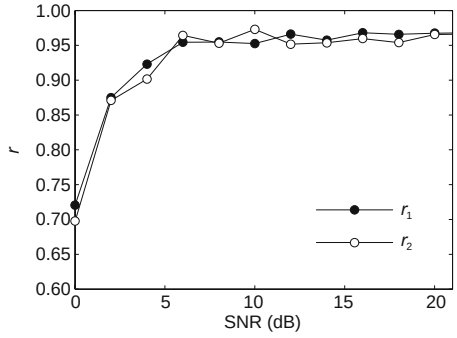

Fig. 10 Cross-correlation coefficients between x_i and the corresponding IMFs decomposed using the centroid-based sifting method

6 Remark

In most real applications, where t and x represent data of the same kind with the same units, the algorithm formulated by Eq. (3) can be applied directly. Occasionally, one might deal with dilations of dependent variable x and independent variable t in such a form as $x\to\alpha x$, and $t\to\beta t$, where α and β are magnifications for x and t, respectively. We note that, by directly using the 'centroids' described above, the decomposition may be non-covariant under the transformation. In mechanics, there is no problem, since the dilation is always isotropic both in the t- and x-directions (i.e., $\alpha=\beta$), and thus, the slope $x'(t)$ in Eq. (3) is invariant. For a signal, the situation may be different, since $\alpha\neq\beta$ in general, say, $\beta=1$ but $\alpha\neq 1$. Let $\mathrm{IMF}_i[x]$ denote the ith IMF extracted from the signal x. Then we have $\mathrm{IMF}_i[\alpha x]\neq\alpha\cdot\mathrm{IMF}_i[x]$.

Under this circumstance, the algorithm can be remedied by replacing the slope $x'(t)$ in Eq. (3) with $\xi'(t)$, where $\xi(t)=x(t)/\sqrt{\int x^2(t)\mathrm{d}t}$, the normalized $x(t)$, so that covariance is preserved, i.e., $\bar{x}_k\to\alpha\bar{x}_k$. To illustrate this, Fig. 11a shows the 'centroids' of the following highly non-symmetrical signal:

$$x(t)=\exp\Big(\cos(2\pi t)+\cos(2\pi\frac{10}{3}t)\Big), \tag{9}$$

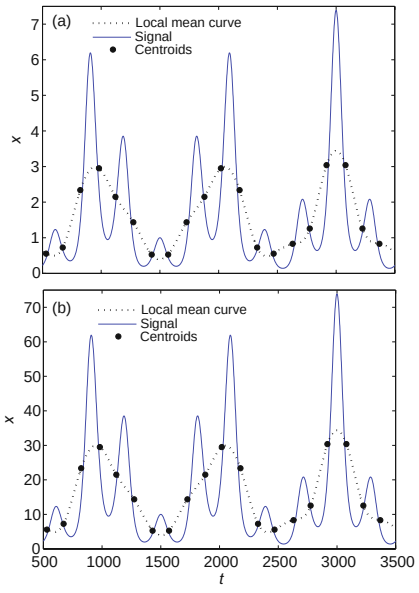

Fig. 11 (a) Local 'centroids' of the non-symmetric signal $x(t)$ as given in Eq. (9); (b) Local 'centroids' of the signal $10x(t)$

and Fig. 11b shows those of the signal that is 10 times amplified. The former are calculated directly from Eq. (3), while the latter are obtained via the preprocessing just described. The dotted lines are the local mean curves interpolating the centroids by the cubic spline. Evidently, we exactly have $\bar{x}(t) \to 10\bar{x}(t)$ by the amplification, and therefore, $\mathrm{IMF}_i[10x] = 10\mathrm{IMF}_i[x]$.

7 Conclusions

In summary, we present a novel sifting method based on local 'centroids' for empirical decomposition of intrinsic mode functions. A local 'centroid' is the integral center of a local signal segment between a pair of local extrema of a signal $x(t)$. It should represent the local mean value more reasonably, and thus the centroids-connected smooth curve should better estimate the local mean curve $\bar{x}(t)$. Indeed, we have shown that the 'centroid'-based sifting greatly mitigates the effect of mode mixing, and is capable of decomposing the intrinsic oscillations with a frequency ratio even up to 0.8, significantly enhancing the frequency resolving power.

An added benefit is the robustness of the new sifting method in processing noisy signals. As given by Eq. (3), local centroids are calculated through local integrations. Therefore, the sifting can resist, to a certain degree, against the noise disturbance by canceling out noises in local signal segments, thus making the sifting process more stable.

References

Cohen, L., 1989. Time-frequency distributions—a review. *Proc. IEEE*, **77**(7):941-981. [doi:10.1109/5.30749]

Datig, M., Schlurmann, T., 2004. Performance and limitations of the Hilbert-Huang Transformation (HHT) with an application to irregular water waves. *Ocean Eng.*, **31**(14-15):1783-1834. [doi:10.1016/j.oceaneng.2004.03.007]

Deering, R., 2006. Final-Scale Analysis of Speech Using Empirical Mode Decomposition: Insight and Applications. PhD Thesis, Duke University, Durham, America.

Deering, R., Kaiser, J.F., 2005. The Use of a Masking Signal to Improve Empirical Mode Decomposition. Proc. IEEE ICASSP, **4**:485-488. [doi:10.1109/ICASSP.2005.1416051]

Hlawatsch, F., Boudreaux-Bartels, G.F., 1992. Linear and quadratic time-frequency signal representation. *IEEE Signal Process. Mag.*, **9**(2):21-67. [doi:10.1109/79.127284]

Huang, N.E., Wu, Z., 2007. An adaptive data analysis method for nonlinear and nonstationary time series: the empirical mode decomposition and Hilbert spectral analysis. *Wavelet Anal. Appl.*, **1**(4):363-376. [doi:10.1007/978-3-7643-7778-6_25]

Huang, N.E., Shen, Z., Long, S.R., Wu, M.C., Shih, H.H., Zheng, Q., Yen, N.C., Tung, C.C., Liu, H.H., 1998. The empirical mode decomposition and the Hilbert spectrum for nonlinear non-stationary time series analysis. *Proc. Roy. Soc. A*, **454**(1971):903-995.

Huang, N.E., Shen, Z., Long, S., 1999. A new view of nonlinear water waves: the Hilbert Spectrum. *Ann. Rev. Fluid Mech.*, **31**:417-459. [doi:10.1146/annurev.fluid.31.1.417]

Huang, N.E., Chern, C.C., Huang, K., Salvino, L.W., Long, S., Fan, K.L., 2001. A new spectral representation of earthquake data: Hilbert spectral analysis of Station TCU129, Chi-Chi, Taiwan, 21 September 1999. *Bull. Seismol. Soc. Am.*, **91**(5):1310-1338. [doi:10.1785/0120000735]

Kopsinis, Y., McLaughlin, S., 2008a. Investigation and performance enhancement of the empirical mode decomposition method based on a heuristic search optimization approach. *IEEE Trans. Signal Process.*, **56**(1):1-13. [doi:10.1109/TSP.2007.901155]

Kopsinis, Y., McLaughlin, S., 2008b. Improved EMD using doubly-iterative sifting and high order spline interpolation. *EURASIP J. Adv. Signal Process.*, **2008**:1-8. [doi:10.1155/2008/128293]

Laila, D.S., Messina, A.R., Pal, B.C., 2009. A refined Hilbert-Huang transform with applications to interarea oscillation monitoring. *IEEE Trans. Power Syst.*, **24**(2):610-620. [doi:10.1109/TPWRS.2009.2016478]

Liang, H., Lin, Z., McCallum, R.W., 2000. Artifact reduction in electrogastrograms based on the empirical mode decomposition. *Med. Biol. Eng. Comput.*, **38**(1):35-41. [doi:10.1007/BF02344686]

Messina, A.R., 2009. Inter-Area Oscillations in Power Systems: a Nonlinear and Nonstationary Perspective. Springer, Berlin, Germany. [doi:10.1007/978-0-387-89530-7]

Rilling, G., Flandrin, P., 2008. One or two frequencies? The empirical mode decomposition answers. *IEEE Trans. Signal Process.*, **56**(1):85-95. [doi:10.1109/TSP.2007.906771]

Schlurmann, T., Dose, T., Schimmels, S., 2001. Characteristic Modes of the 'Adreanov Tsunami' Based on the Hilbert-Huang Transformation. Proc. 4th Int. Symp. on Ocean Wave Measurement and Analysis, **2**:1525-1534. [doi:10.1061/40604(273)154]

Senroy, N., Suryanarayanan, S., Ribeiro, P.F., 2007. An improved Hilbert-Huang method for analysis of time-varying waveforms in power quality. *IEEE Trans. Power Syst.*, **22**(4):1843-1850. [doi:10.1109/TPWRS.2007.907542]

Xuan, B., Xie, Q., Peng, S., 2007. EMD sifting based on bandwidth. *IEEE Signal Process. Lett.*, **14**(8):537-540. [doi:10.1109/LSP.2007.891833]